

A Dual-Exposure In-Pixel Charge Subtraction CTIA CMOS Image Sensor for Centroid Measurement in Star Trackers

Xinyuan Qian¹, Menghan Guo¹, Hang Yu¹, Shoushun Chen² and Kay Soon Low¹

¹Satellite Research Center, ²VIRTUS IC Design Center of Excellence,
Nanyang Technological University, Singapore

Abstract—In this work, we present a CMOS image sensor for star centroid measurement in star trackers. The analysis of the star tracker system shows that long integration will cause "tail effect" in the star image. It significantly reduces the signal magnitude, which in turn increases the centroiding errors. In order to capture limited photons generated from dim stars within shortened integration time, we propose a new capacitive transimpedance amplifier (CTIA) pixel architecture with a small integration capacitor. On the other hand, bright stars can easily saturate the pixels, which can also induce significant measurement errors. To avoid pixel saturation, the pixel is able to perform in-pixel charge subtraction based on photocurrent thresholding. In order to validate the pixel design, we have fabricated a test chip consisting of a 4×4 pixel array using Global Foundry 65 nm mixed signal CMOS process.

I. INTRODUCTION

A star tracker is an optical-electronic device to produce the 3-axis attitude information of a spacecraft by observation of the star field. It can achieve an angular accuracy in the range of arcseconds [1] and currently is the most accurate among all existing attitude sensors. Fig. 1 illustrates the diagram of a typical star tracker, which is composed of an image sensor and associated signal processing electronics. The image sensor first captures a star field. Centroids of the stars are then computed to build a star pattern. After that, the pattern is passed to a recognition algorithm to determine the attitude [2].

The recognition accuracy has a strong dependence on the precision of the star centroids. Due to satellite orbit, a short exposure time is preferred to achieve the desired accuracy. However, shorter exposure time implies higher requirement on the sensitivity and signal to noise ratio. High dynamic range is equally important in this application. A typical star tracker has can detect six visual magnitude levels, which means a dynamic range of more than 90 dB with acceptable SNR. High dynamic range allows to capture both very bright and dark stars in the same scene.

In this work, we propose a CMOS image sensor for star tracker. The effects of the pixel sensitivity and dynamic range on the measurement of star centroid are discussed. We propose a new pixel architecture that is capable of provide both high sensitivity and high dynamic range. The rest of the paper is organized as follows: Section II introduces system analysis of the sensor design. Section III describes the sensor architecture and

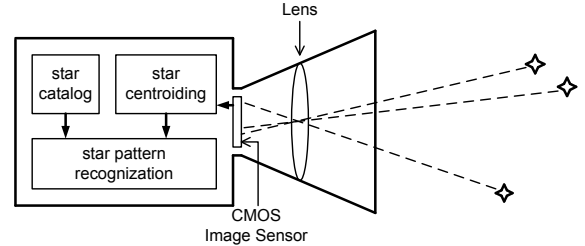


Fig. 1. Block diagram of a typical star tracker.

pixel circuits. Section IV describes the sensor implementation and measurement results. Conclusions are drawn in Section V.

II. SYSTEM ANALYSIS

Stars generate limited number of photons on the focal plane. Using the Sun ($M_V = -26.76$ and solar flux of 1.3 kW/m^2) as reference, we can derive any other star's luminance. By taking into such factors as luminance spectral distribution, photo-detector's quantum efficiency (QE) and lens point spread function (PSF), it is possible to estimate the number of generated photons received by the sensor. For a star tracker with 3 cm lens aperture, 85% lens transmission efficiency, 1 pixel PSF, and 50 ms exposure time, a $M_V = 6$ star can only generate about 300 photoelectrons at the center pixel of the star [3]. This is challenging for CMOS image sensor, in particular, under space radiation environment.

However, increasing the integration time is not helpful in star tracker. In fact, longer exposure time leads to systematic error due to the satellite orbiting, which is shown in Fig. 2. The orbital movement of the satellite causes the star image to drift in reverse direction on the focal plane. The shift distance (L) can be expressed as:

$$L = \frac{N_{pix} \cdot \omega \cdot T_{int}}{2 \tan(FOV/2)} (\text{pixels}) \quad (1)$$

where N_{pix} is the pixel number in one dimension of the pixel array, ω is the angular rate, T_{int} is the integration time and FOV is the field of view of the star tracker. A low-earth orbit (LEO) satellite at the altitude of 600 km has an angular rate of 0.06 deg/s. For a CMOS image sensor with 1000 pixels in one dimension and 20 deg FOV , 100 ms integration time can produce a shift of 0.3 pixel. The center of the star will shift to other pixels and the incident photons will spread over more

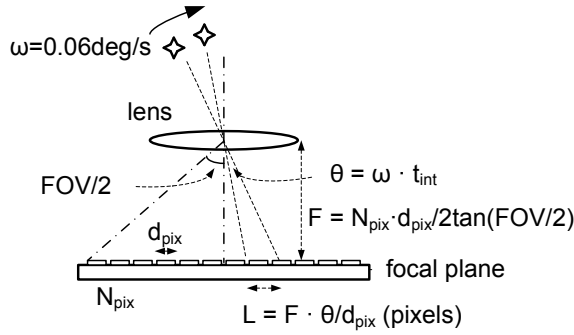


Fig. 2. Systematic error due to satellite orbit: stars travel on the focal plane. The travel distance L is expressed in pixels in one dimension, where d_{pixel} is the pixel pitch.

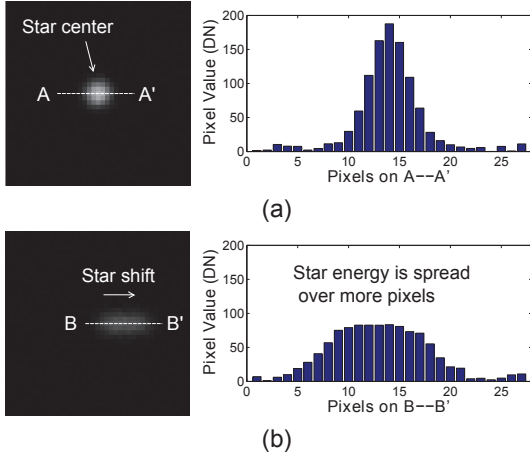


Fig. 3. (a) shows simulated star images and its pixel responses along A-A' with no shift distance, respectively. (b) shows simulated star images and its pixel responses along B-B' with shift distance, respectively. They are captured with the same integration time. Tail effect is obvious which reduces the signal magnitude significantly.

pixels when integration time is further increased. This forms the "tail effect". Fig. 3 shows the simulated star images under both static and dynamic condition. In dynamic condition, the shift causes the star energy to spread over more pixels but is not beneficial for increasing signal magnitude.

Therefore, for improved centroiding accuracy, the image sensor should be a global shutter. It is necessary to increase the sensitivity against the shortened exposure time. Although, high sensitivity can easily cause bright stars to saturate [4],

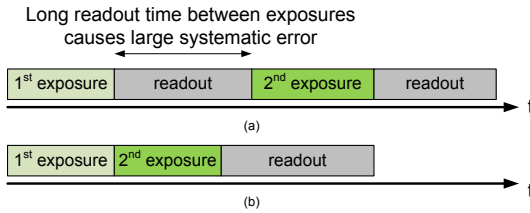


Fig. 4. Global-shutter timing difference between (a) conventional and (b) proposed dual-exposure high dynamic range method. In conventional method, there is a frame readout between two exposures. The readout time can be several milliseconds long. For example, 100 ms is expected if we assume an array of 2M pixels with 20MHz clock frequency. It causes a shift of 0.3 pixels on focal plane between two exposures, which adds to the centroiding error.

which again causes centroiding error. The extension of dynamic range is thus required. As a result, the solution to all the contradictions is a CMOS image sensor with both high sensitivity and high dynamic range. We propose a new sensor architecture based on CTIA pixel [5][6][7] for high sensitivity. High dynamic range is achieved by a dual-exposure in-pixel charge subtraction scheme. The first exposure measures the light intensity with a saturation threshold and if saturation is found, a packet of charges is subtracted from the integration results during the second exposure. The resulting effective well capacity is increased and a wider range of photocurrent can be quantized. As shown in Fig.4, the scheme differs from the conventional method in that there is no readout time in two exposures, which would otherwise be long due to large pixel array. This will minimize the systematic error and is better suited for this application.

III. IMAGE SENSOR DESIGN

A. Pixel Circuit

The schematic of the pixel circuits is shown in Fig.5. Fig.5 (a) illustrates the functional block diagram of the pixel architecture. The pixel has an integrator to accumulate the photocurrent. The output of the integrator (V_o) of the first exposure is compared with a threshold reference to denote whether the pixel is saturated. Its result is latched in the DFF and used to decide whether to apply charge subtraction in the consecutive second exposure. If the pixel is saturated, an externally-produced voltage (V_{sub}) is subtracted from V_o .

The pixel consists of a photodiode, an operational transconductance amplifier (OTA), a reset switch, switched-capacitor circuits, a comparator with latch and a clamp circuit followed by a source follower for readout. The photodiode, the OTA, the reset switch and the integration capacitor C_{int} , forms the fundamental CTIA pixel, whereas the OTA, C_{int} and C_{sub} constitutes the circuit for charge subtraction. The clamp circuit is used for in-pixel Correlated Double Sampling (CDS). The source follower drives the column bus when the row is selected.

In CTIA pixel, the photodiode voltage is held at a constant value by the OTA so the photocurrent (I_{ph}) will flow to discharge the integration capacitor. The output follows:

$$V_o \approx \frac{1}{C_{int}} \int I_{ph} dt \quad (2)$$

The schematic of the OTA (Fig. 5(b)) is a single-ended cascode common-source amplifier. The reset switch (Fig. 5(c)) consists of three NMOS transistors and an inverter instead of one simple NMOS transistor. During integration, the node between $M1$ and $M2$ is tied to an externally-produced bias voltage (V_{im}) close to V_i . So the leakage path from V_o to V_i is eliminated when V_o builds up. The comparator (Fig. 5(d)) is a five-transistor OTA used in open-loop configuration followed by a digital buffer.

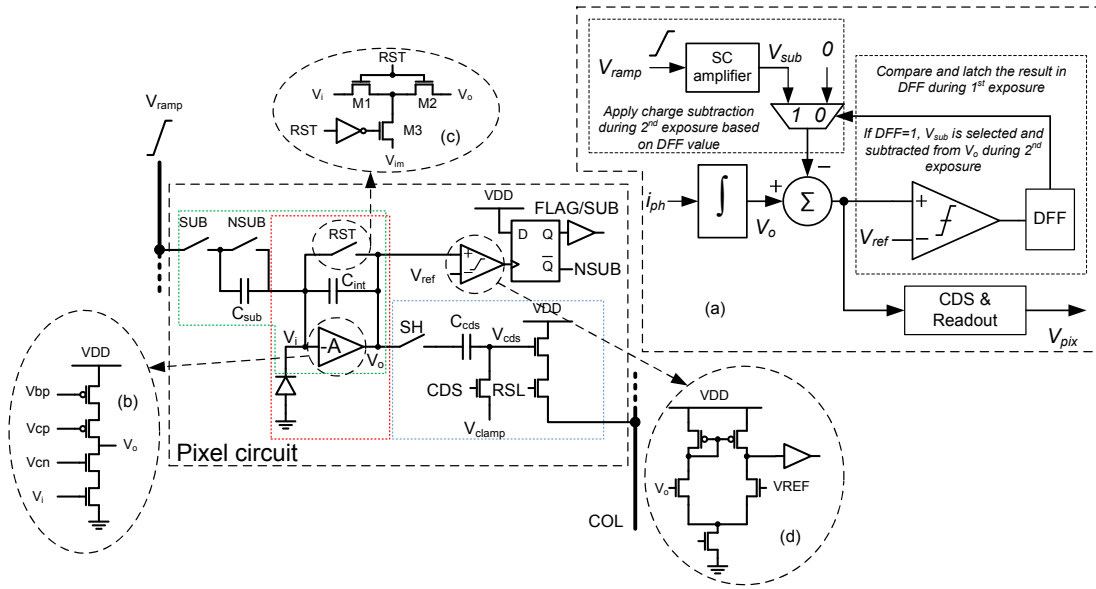


Fig. 5. The schematic of the pixel circuit. (a) Pixel functional block diagram, (b) the schematic of the OTA, (c) the reset switch and (d) the comparator are shown respectively.

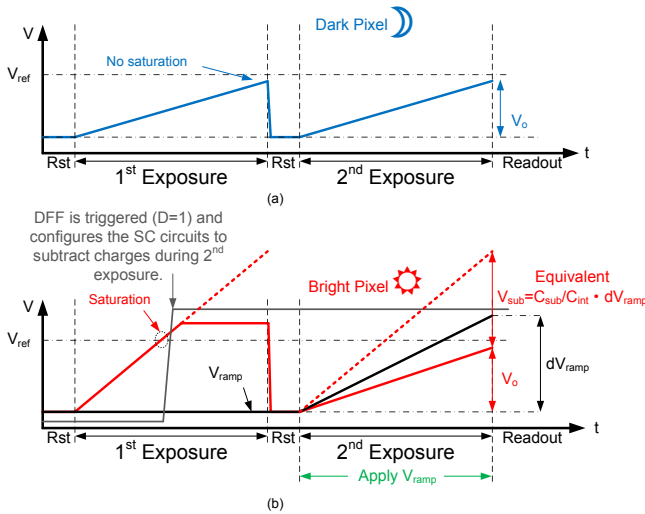


Fig. 6. Pixel operation timing diagram.

B. Pixel Operation

Fig. 6 shows the timing diagram of the pixel circuit. The pixel operation features two identical-length exposure and the scheme of charge subtraction based on the photocurrent evaluation in the first one. The pixel can be self-configured based on the photocurrent thresholding result. The details of the pixel operation is described as follows.

The pixel is reset before each exposure. At the same time, the transistor controlled by CDS is turned on. After that, it is turned off a short delay after reset switch is turned off. In this manner, the reset level of the OTA, including negative charge injection of reset switch, the reset noise and OTA offset is clamped onto C_{cds} .

During the first exposure, if the photocurrent is small and the

integration result does not reach the voltage threshold defined by V_{ref} , as the case in Fig. 6(a), the comparator will not toggle and trigger the D-type register. Hence, both exposures have the same response. The photocurrent can be simply expressed as:

$$I_{ph} = \frac{C_{int} \cdot V_o}{T_{int}} \quad (3)$$

Once integration result reaches the voltage threshold and comparator toggles, as the case in Fig. 6(b), the outputs of the register are used to reconfigure the switches associated with C_{sub} . It connects C_{sub} to a column bus driven by a ramp signal (V_{ramp}). During the second integration period, the ramp signal starts to rise as the integration starts. The photocurrent can then be expressed as:

$$I_{ph} = \frac{C_{int} \cdot V_o + C_{sub} \cdot dV_{ramp}}{T_{int}} \quad (4)$$

Since the DFF stores the information whether the pixel conducts charge subtraction, the pixel outputs both analog voltage (V_o) and one-bit digital signal for image reconstruction.

IV. PROTOTYPE CHIP AND MEASUREMENT RESULTS

Fig. 7(a) shows the test setup with the prototype chip. The sensor is illuminated by back-lit point sources in a dark room. Fig. 7(b) and (c) shows the prototype chip and pixel layout implemented using 3.3 V devices with Global Foundries 65 nm CMOS mixed-signal process, respectively. The array contains 4×4 pixels, which is sufficient to evaluate its accuracy in star centroid measurement. The peripheral circuits include a row scanner, a column scanner and a global analog buffer (not shown). The pixel is $22 \times 22 \mu\text{m}^2$ and uses a $10.8 \mu\text{m} \times 5.9 \mu\text{m}$ N-well/P-sub photodiode with a parasitic capacitance of about 40fF. All in-pixel capacitors are MIM capacitors. C_{int} and C_{sub} are equally designed to be about 10 fF, which gives

TABLE I
PERFORMANCE SUMMARY OF THE SENSOR

Technology	Global Foundry 65 nm mixed-signal CMOS
Pixel Size	$22 \times 22 \mu\text{m}^2$ (Fill Factor: 14%)
Conversion Gain	$16 \mu\text{V}/\text{e}^-$
Signal Swing	160mV - 1.4V
Sensitivity	$3.8 \text{ V}/\text{lux}\cdot\text{s}$
Dark Current	48 fA
Temporal Noise	$980 \mu\text{V}$ (61 e ⁻)
Linearity	$\pm 0.57\%$
Well Capacity	77500 e ⁻ (265000 e ⁻ with charge subtraction)
Dynamic Range	62 dB (74 dB with charge subtraction)

a CTIA gain of about four. In order to improve inter-capacitor matching, C_{sub} and C_{int} are placed next to each other and active devices are placed away from the capacitors. The value of C_{cds} is selected to be 28 fF.

Fig. 8 shows the measured photocurrent with regard to incident light intensity. With 1 ms integration time, the pixel saturates at about 300 lux. After performing charge subtraction, the pixel saturates at around 1100 lux. This amounts to approximately 12 dB increase of the dynamic range. The sensitivity is $3.8 \text{ V}/\text{lux}\cdot\text{s}$ with conversion gain of $16 \mu\text{V}/\text{e}^-$. The readout noise seen at the output is about 0.98 mV_{rms} . Chip characteristics are summarized in Table I.

Point sources are used to simulate "star" signals. We apply centroiding algorithm in [3] to assess the centroiding accuracy. The point sources are projected onto the centers of the pixel A, B and C alternatively, as shown in Fig. 7(b). The three centroids are calculated and their measured distance AB and AC are compared. Fig. 9 shows this measured distance error at different integration time. The centroiding accuracy increases with exposure time since the accuracy benefits from the increased signal magnitude and its SNR. After about 80 ms exposure in this test, the "star" pixels begin to saturate gradually. No further obvious improvement on centroiding accuracy is observed since the photocurrent measurement is distorted. But with the charge subtraction, the pixel still can quantize the photocurrent until about 120 ms and the centroiding accuracy continues increasing.

V. CONCLUSION

The design of a centroid measurement CMOS image sensor for star trackers is described. For accurate starlight measurement in shortened integration time, a new CTIA pixel architecture is proposed. In order to increase the centroiding

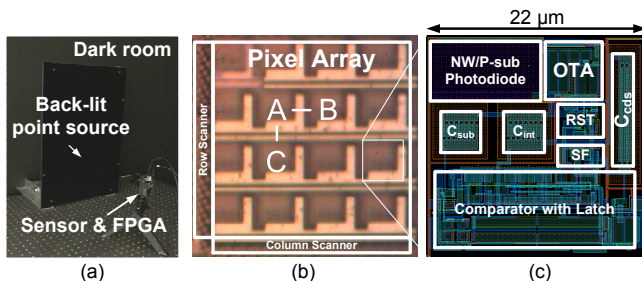


Fig. 7. (a) Test setup, (b) prototype chip microphotograph and (c) pixel layout.

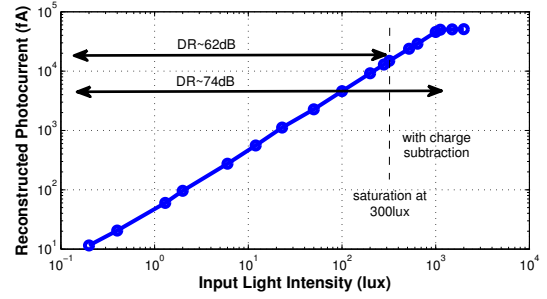


Fig. 8. Measured photocurrent with regard to incident light intensity. The pixel saturates at around 300 lux. With charge subtraction, the dynamic range increases by approximately 12dB and saturates at around 1100 lux.

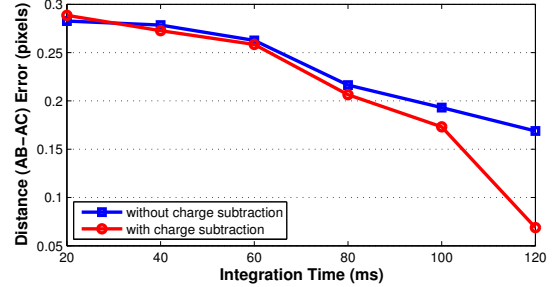


Fig. 9. Measured $AB - AC$ distance error at different integration times. Saturation occurs in "stars" after about 80 ms. But with charge subtraction, centroiding accuracy improves much better compared with saturated one.

accuracy of bright stars that can easily cause saturation, the pixel features a scheme of pixel-level charge subtraction. It allows the pixel to conduct charge subtraction decided by photocurrent thresholding in two consecutive exposures. A proof-of-concept chip consisting of a 4×4 pixel array is fabricated in Global Foundry 65 nm mixed-signal CMOS process.

VI. ACKNOWLEDGEMENT

This work is supported by ACRF Project(M4020153.040).

REFERENCES

- [1] C. Liebe, L. Alkalai, G. Domingo, B. Hancock, D. Hunter, J. Mellstrom, I. Ruiz, C. Sepulveda, and B. Pain, "Micro APS based star tracker," in *2002. IEEE Aerospace Conference Proceedings*, vol. 5, 2002, pp. 5–2285–5–2299 vol.5.
- [2] M. Pham, K.-S. Low, and S. Chen, "An Autonomous Star Recognition Algorithm with Optimized Database," *IEEE Transactions on Aerospace and Electronic Systems*, vol. 49, no. 3, pp. 1467–1475, 2013.
- [3] C. Liebe, "Accuracy Performance of Star Trackers - A Tutorial," *IEEE Transactions on Aerospace and Electronic Systems*, vol. 38, no. 2, pp. 587–599, apr 2002.
- [4] X. Qian, H. Yu, S. Chen, and K. Low, "An Adaptive Integration Time CMOS Image Sensor With Multiple Readout Channels," *IEEE Sensors Journal*, vol. 13, no. 12, pp. 4931–4939, 2013.
- [5] S. Kavusi, K. Ghosh, and A. El Gamal, "A Per-Pixel Pulse-FM Background Subtraction Circuit with 175ppm Accuracy for Imaging Applications," in *IEEE International Solid-State Circuits Conference, 2007. ISSCC 2007. Digest of Technical Papers.*, 2007, pp. 504–618.
- [6] K. Murari, R. Etienne-Cummings, N. Thakor, and G. Cauwenberghs, "A CMOS In-Pixel CTIA High-Sensitivity Fluorescence Imager," *IEEE Transactions on Biomedical Circuits and Systems*, vol. 5, no. 5, pp. 449–458, 2011.
- [7] R. Xu, B. Liu, and J. Yuan, "A 1500 fps Highly Sensitive 256 X 256 CMOS Imaging Sensor With In-Pixel Calibration," *IEEE Journal of Solid-State Circuits*, vol. 47, no. 6, pp. 1408–1418, 2012.